

# The mitral annulus in transposition of the great arteries late after Senning- and Mustard-procedures (Insights from the CSONGRAD Registry and MAGYAR-Path Study)

Attila Nemes, Árpád Kormányos

Department of Medicine, Albert Szent-Györgyi Medical School, University of Szeged, Szeged, Hungary

*Contributions:* (I) Conception and design: A Nemes; (II) Administrative support: Á Kormányos; (III) Provision of study materials or patients: A Nemes; (IV) Collection and assembly of data: Á Kormányos; (V) Data analysis and interpretation: Both authors; (VI) Manuscript writing: Both authors; (VII) Final approval of the manuscript: Both authors.

*Correspondence to:* Attila Nemes, MD, PhD, DSc, FESC. Department of Medicine, Albert Szent-Györgyi Medical School, University of Szeged, Semmelweis Street 8, H-6725 Szeged, Hungary. Email: nemes.attila@med.u-szeged.hu.

**Introduction:** Dextro-transposition of the great arteries (dTGA) is a rare condition comprising 5–7% of all congenital heart diseases (CHD). Until 1990s, atrial switch operations were the method of choice for the treatment of dTGA. The aim of our present study was to evaluate the abnormalities of the mitral annulus (MA) by three-dimensional speckle-tracking echocardiography (3DSTE). Potential differences in MA dimensions and functional properties late after Senning- and Mustard-procedures were analyzed as well.

**Methods:** This retrospective cohort study comprised 19 dTGA patients late after atrial switch operation, from which 7 subjects were not involved due to inferior image quality. The remaining dTGA patient group comprised 12 subjects (age: 30.7±8.6 years, 7 males). For comparisons, 32 age- and gender-matched healthy controls were evaluated (age: 34.4±12.3 years, 18 males).

**Results:** End-systolic and end-diastolic MA diameter (MAD), area and perimeter proved to be increased, while MA functional parameters [MA fractional area change (MAFAC) and fractional shortening (MAFS)] were reduced in all dTGA patients as compared to matched controls regardless of the atrial switch procedure used. However, MA morphological parameters were tendentially lower, while MA functional parameters were tendentially favorable in case of Senning-procedure compared to Mustard-procedure.

**Conclusions:** dTGA is accompanied by MA dilation and its functional impairment late after Senning- and Mustard-procedures.

**Keywords:** Dextro-transposition of the great arteries (dTGA); mitral annulus (MA); three-dimensional; speckle-tracking; echocardiography

Submitted Apr 25, 2022. Accepted for publication Aug 10, 2022.

doi: 10.21037/cdt-22-208

View this article at: <https://dx.doi.org/10.21037/cdt-22-208>

## Introduction

Although dextro-transposition of the great arteries (dTGA) is a rare pathological state, it is one of the most common cyanotic congenital heart diseases (CHD) (1-3). In dTGA, the aorta and the pulmonary artery (PA) are swapped over (switched), the aorta originates from the anterior morphologically right ventricle (RV), while the PA emerges

from the posterior morphologically left ventricle (LV) (1-3). Until the 1990s, atrial switch operations (Senning- and Mustard-procedures) were the method of choice for the treatment of dTGA, then the more physiological arterial switch operation became the corrective operation (4-6). With the Senning-procedure, a baffle is created within the atria that directs blood flow from the caval veins to the

pulmonary circulation via the mitral valve (MV) and the LV. The Mustard-procedure is an alternative technique, when following excision of the atrial septum, prosthetic tissue is used for the creation of the atrial baffle. However, regardless of which atrial switch procedure was used, original pathological states at ventricular level remained uncorrected with the RV functioning as the systemic ventricle (4-6).

The MV plays a crucial role in regulating normal blood flow. Its annulus (MA), however, could be deformed, enlarged and functionally impaired due to internal and/or external circumstances (7). Three-dimensional speckle-tracking echocardiography (3DSTE) non-invasively estimates MA dimensions in addition to chamber quantifications (8-12). Theoretically, dTGA and its correction with atrial switch is associated with volumetric and functional alterations of cardiac chambers including LV and left atrium (LA) remodeling. In most cases, abnormalities of left (and right) atria and ventriculi are accompanied with dilation and functional impairment of atrioventricular annuli between them, as demonstrated before in other disorders (12). Due to the presence of dTGA-associated special pathological state following atrial switch, the present retrospective cohort study aimed non-invasive assessment of MA dimensions and functional properties by 3DSTE. Potential differences in MA sizes and functional parameters in patients late after Senning- and Mustard-procedures were investigated as well. We present the following article in accordance with the STROBE reporting checklist (available at <https://cdt.amegroups.com/article/view/10.21037/cdt-22-208/rc>).

## Methods

### *Patient population*

Detailed parameters of demographic data, risk factors, disorders, drugs used, procedure(s) carried out and echocardiographic data of CHD patients were collected into a dedicated registry called as CSONGRAD Registry (Registry of C(S)ONGenital caRdiAc Disease patients at the University of Szeged) at our tertiary center, and data of dTGA patients were analysed from this registry (13). From 196 dTGA patients, who underwent non-arterial procedures, Senning-procedure was the method of atrial switch in 37 patients, while Mustard-procedure was used in 48 patients between 1961–2013 (14). The study comprised 19 dTGA patients late after atrial switch operation, from which 7 subjects were excluded due to inferior image

quality. The remaining dTGA patient group consisted of 6 Senning-operated and 6 Mustard-operated subjects (mean age of  $30.7 \pm 8.6$  years, 7 males) (*Figure 1*). For comparisons, 32 healthy controls were involved who were matched for age and gender (mean age:  $34.4 \pm 12.3$  years, 18 males). Data of controls were selected from the data pool of healthy controls. A subject was considered to be healthy in the absence of any disorder, pathological state, drug use or any case which could affect the results. Moreover, laboratory, routine electrocardiographic and echocardiographic findings proved to be normal. The Motion Analysis of the heart and Great vessels bY three-dimensional speckle-tRacking echocardiography in Pathological cases (MAGYAR-Path) Study was organized at our department for detailed assessment of diagnostic and prognostic significance of 3DSTE-derived parameters in different pathological states including dTGA ('Magyar' means 'Hungarian' in Hungarian language) (15-17). Data collection was completed in 2019. The study was conducted in accordance with the Declaration of Helsinki (as revised in 2013). The study was approved by the Institutional and Regional Human Biomedical Research Committee of University of Szeged, Hungary (No. 71/2011) and informed consent was taken from all individual participants.

### *2D Doppler echocardiography*

Toshiba Artida™ echocardiographic tool (Toshiba Medical Systems, Tokyo, Japan) attached with a PST-30BT (1–5 MHz) phased-array transducer was used for 2D Doppler echo. The measured 2D echocardiographic parameters included LA diameter, thicknesses of interventricular septum (IVS) and LV posterior wall and end-systolic and end-diastolic LV diameters and volumes (all measured in parasternal long-axis view), which were assessed together with visual continuous Doppler evaluation of valvular regurgitations and pulsed Doppler-based exclusion of valvular stenoses (18).

### *3DSTE*

Following 3D echocardiographic data acquisitions, an offline analysis was performed at a later date (8-11). Firstly, the same Toshiba Artida™ echocardiographic tool (Toshiba Medical Systems) was used attached with a PST-25SX matrix-array transducer with 3D capability for the collection of an 'echocloud' from the apical window within a single

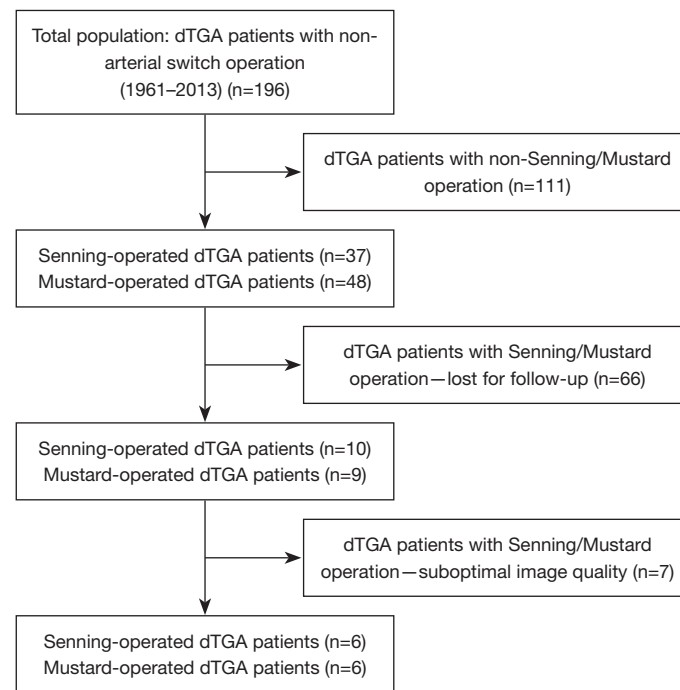


**Figure 1** Flowchart of the study with the total population and exclusions due to non-Senning-or Mustard-procedures, lost for follow-up and suboptimal image quality. dTGA, dextro-transposition of the great arteries.

breath-hold for patients being in sinus rhythm. Routinely, 6 wedge-shaped subvolumes were collected within 6 cardiac cycles, then a pyramid-shaped 3D full volume was created where the measurements were performed.

For MA parameters, due to absence of automatic software analysis for annular measurements, all the analysis was done manually according to our practice by the same doctor (ÁK). Following image plane optimizations on the endpoints of the MA on non-foreshortened AP2CH and AP4CH views, the following measurements were performed in end-diastole and end-systole on the C7 short-axis view (Figure 2) (12,19,20):

- ❖ MA diameter (MAD) was measured by drawing a perpendicular line from the peak of MA curvature to the middle of the straight MA border at end-diastole and end-systole as well.
  - ❖ MA area (MAA) was assessed by planimetry.
  - ❖ MA perimeter (MAP) was assessed by planimetry.
- MA functional properties were measured using MA dimensions:
- ❖ MA fractional shortening (MAFS) =  $(\text{end-diastolic MAD} - \text{end-systolic MAD}) / \text{end-diastolic MAD} \times 100$
  - ❖ MA fractional area change (MAFAC) =  $(\text{end-diastolic MAA} - \text{end-systolic MAA}) / \text{end-diastolic MAA} \times 100$

For LA/LV parameters, virtual casts of these chambers were created by the same observer at the same time. Following image optimization, LA/LV endocardial border was detected by setting several markers from the septum-MA edge towards LA/LV lateral wall-MA edge. Then automatic reconstruction of the LA/LV endocardial surface was performed allowing LA/LV strain analyses.

### Statistical analysis

Data were given as frequencies and percentages if proved to be categorical and expressed as mean  $\pm$  standard deviation if proved to be continuous. Differences were considered to be statistical significant if  $P < 0.05$ . All tests were two-sided. Categorical variables were assessed by Fisher's exact test. Bland and Altman's method was used for studying intra- and interobserver agreement. Pearson's coefficient was used for correlation between variables. Normality of distribution was tested for continuous variables with Shapiro-Wilks test: Student's *t*-test was used in the presence of normal distribution and Mann-Whitney-Wilcoxon test was performed in the presence of non-normal distribution. Medcalc software package was used for statistical analysis (Medcalc, Mariakerke, Belgium).

**Table 1** Clinical and two-dimensional echocardiographic data of patients with dTGA and controls at baseline

Data	Controls (n=32)	dTGA patients (n=12)
Clinical data		
Age (years)	34.4±12.3	30.7±8.6
Male gender	18 [56]	7 [58]
Hypertension	0	3 [19]*
Diabetes mellitus	0	0
Hypercholesterolemia	0	0
Two-dimensional echocardiography		
LA-D (mm)	37.5±3.7	34.9±5.9
LV-ED-D (mm)	48.4±3.8	47.0±5.1
LV-ED-V (mL)	107.9±30.6	111.0±23.4
LV-ES-D (mm)	38.0±19.6	30.2±4.3
LV-ES-V (mL)	33.0±3.8	39.1±11.5
IVS (mm)	8.8±1.4	10.0±1.8*
LV-PW (mm)	9.0±1.2	9.9±1.5
LV-EF (%)	65.8±4.8	62.6±6.6

\*,  $P < 0.05$  vs. controls. dTGA, dextro-transposition of the great arteries; LA, left atrial; D, diameter; LV, left ventricular; ED, end-diastolic; V, volume; ES, end-systolic; EF, ejection fraction; IVS, interventricular septum; PW, posterior wall.

## Results

### Clinical and demographic data

Data are presented in *Table 1*. From the classical risk factors, only hypertension was present in some dTGA patients. Atrial septal defect, ventricular septal defect and patent ductus arteriosus could be detected in 2, 3 and 4 cases with dTGA, respectively. The average age at the time of the first procedure was  $1.5 \pm 1.0$  years in the population of dTGA patients. The average time between 3DSTE and surgery was  $29.4 \pm 8.2$  years in this group of subjects.

### 2D Doppler echocardiography

From 2D echocardiographic data, IVS was thickened in dTGA patients, while other routine LA and LV dimensions and volumes did not differ between dTGA patients and controls (*Table 1*). Grade 1–2 mitral regurgitation (MR) was present in 2 patients, while grade 3–4 MR did not occur.

Grade 1–2 tricuspid regurgitation (TR) could be detected in 5 patients, while grade 3–4 TR was present in 6 dTGA patients. None of the healthy controls showed MR or TR. No significant valvular stenosis could be detected in any valves in any patients and controls.

### 3DSTE

End-systolic and end-diastolic MAD, MAA and MAP proved to be dilated, while MA functional parameters (MAFAC and MAFS) were reduced in all dTGA patients as compared to matched controls regardless of the atrial switch procedure used. However, MA morphological parameters were tendentially lower, while MA functional parameters were tendentially favorable in case of Senning-procedure compared to Mustard-procedure (*Table 2*). Global peak LA longitudinal (LA-LS) and circumferential (LA-CS) strains and LV-LS strain proved to be  $11.9\% \pm 7.1\%$ ,  $10.8\% \pm 9.7\%$  and  $-16.1\% \pm 5.5\%$ , respectively. LA-LS did not show correlation with MAFAC and MAFS ( $r=0.18$ ,  $P=0.34$  and  $r=0.21$ ,  $P=0.31$ ). Similarly, LA-CS did not show correlations with MAFAC and MAFS ( $r=0.16$ ,  $P=0.32$  and  $r=0.19$ ,  $P=0.30$ ). LV-LS did not correlate with MAFAC and MAFS ( $r=0.13$ ,  $P=0.45$  and  $r=0.19$ ,  $P=0.30$ ).

### Intra- and interobserver agreement

Reproducibility of data for MA parameters for dTGA patients are presented together with corresponding correlation coefficients in *Table 3*.

## Discussion

The MV apparatus forms a complex 3D structure involving MA, anterior and posterior leaflets, chordae tendineae and papillary muscle (7). MA has a significant role in this structure with its fibrous, saddle-like (hyperbolic paraboloid) shape helping to bind MV leaflets and surroundings. Moreover, MA constitutes the anatomical junction between the LV and LA helping optimal unidirectional blood flow during diastole. In normal circumstances there is a harmonious interplay between parts of the MV including MA without backflow in systole. In case of improper valvular function, functional MR could develop (7,21,22).

Recent developments in non-invasive cardiovascular imaging allow detailed assessment of atrioventricular valvular dimensions and function. MA can be assessed by 3DSTE, an easy-to-perform method. Assessment of the

**Table 2** Comparison of mitral annular morphological and functional parameters measured with 3DSTE in patients with dTGA and controls

Data	Controls (n=32)	All dTGA patients (n=12)	Senning-operated dTGA patients (n=6)	Mustard-operated dTGA patients (n=6)
Morphological parameters				
MAD-D (cm)	2.58±0.50	2.63±0.31	2.55±0.34	2.77±0.34
MAA-D (cm <sup>2</sup> )	8.13±2.56	9.25±2.71	9.30±3.19	9.67±3.13
MAP-D (cm)	10.78±1.50	11.69±1.74	11.80±2.35	11.95±1.68
MAD-S (cm)	1.60±0.36	2.19±0.38*	2.10±0.40*	2.42±0.27*
MAA-S (cm <sup>2</sup> )	3.81±1.38	6.89±2.57*	6.55±3.42*	7.77±1.95*
MAP-S (cm)	7.50±1.25	10.08±1.82*	9.78±2.31*	10.68±1.34*
Functional parameters				
MAFAC (%)	51.62±14.07	26.00±12.46*	30.98±13.75*	18.45±7.77*
MAFS (%)	37.06±13.58	17.00±9.50*	17.76±9.16*	12.37±7.34*

\*, P<0.05 vs. controls. 3DSTE, three-dimensional speckle-tracking echocardiography; dTGA, dextro-transposition of the great arteries; MA, mitral annulus; MAD-D, end-diastolic MA diameter; MAA-D, end-diastolic MA area; MAP-D, end-diastolic MA perimeter; MAD-S, end-systolic MA diameter; MAA-S, end-systolic MA area; MAP-S, end-systolic MA perimeter; MAFAC, MA fractional area change; MAFS, MA fractional shortening.

**Table 3** Intra- and interobserver variability for mitral annular dimensions

Data	Intraobserver agreement		Interobserver agreement	
	Average ± standard deviation difference in parameters measured 2 times by same examiner	Correlation coefficient between 2 measurements of the same examiner	Average ± standard deviation difference in parameters measured by 2 examiners	Correlation coefficient between measurements of 2 examiners
End-diastolic MAD	0.02±0.25 cm	0.93 (P<0.0001)	0.04±0.21 cm	0.95 (P<0.0001)
End-diastolic MAA	-0.03±1.23 cm <sup>2</sup>	0.95 (P<0.0001)	0.02±0.86 cm <sup>2</sup>	0.95 (P<0.0001)
End-diastolic MAP	-0.04±0.97 cm	0.94 (P<0.0001)	-0.12±0.93 cm	0.94 (P<0.0001)
End-systolic MAD	-0.04±0.21 cm	0.96 (P<0.0001)	0.03±0.25 cm	0.97 (P<0.0001)
End-systolic MAA	-0.03±0.35 cm <sup>2</sup>	0.96 (P<0.0001)	-0.06±0.55 cm <sup>2</sup>	0.97 (P<0.0001)
End-systolic MAP	0.08±0.62 cm	0.96 (P<0.0001)	0.07±0.52 cm	0.97 (P<0.0001)

MAD, mitral annular diameter; MAA, mitral annular area; MAP, mitral annular perimeter.

MA can be performed from the transthoracic apical window by a single echocardiographic data acquisition. With help of 2D-projected images, assessment can be performed in any plane (8-12). 3DSTE was confirmed to have excellent intra- and interobserver agreement in the evaluation of MA dimensions (12).

There are limited information of MV characteristics in dTGA. MV anomalies associated with dTGA were found to be rare but present with consistent anatomic features and there was a higher risk of coarctation following arterial

switch operation (23). This is the first time to assess MA dimensions and functional parameters measured by 3DSTE in patients with corrected dTGA late after atrial switch operation to the best of our knowledge. Although Senning- and Mustard-procedures are 'old-fashioned' procedures now and not used clinically anymore, patients treated with such operations could appear in the clinical practice (1-6). According to the literature, limited information is available regarding to dTGA-associated changes in myocardial mechanics and valvular morphology and

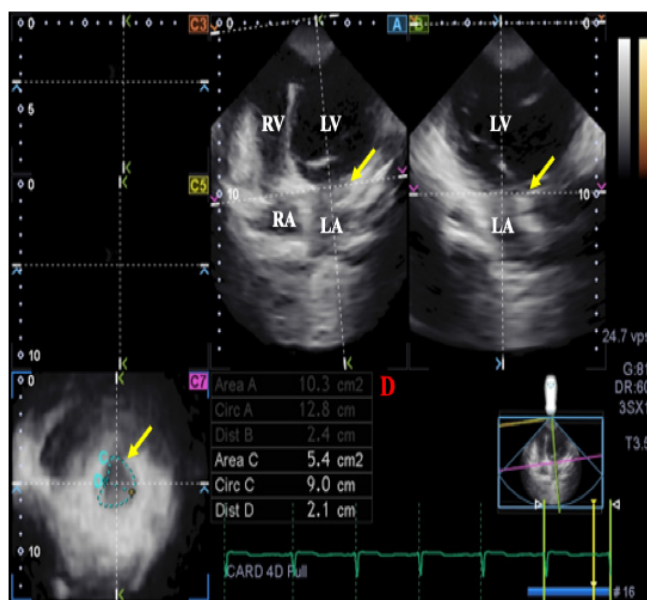


**Figure 2** Images from three-dimensional full-volume dataset showing MA in a patient with dTGA: (A) apical four-chamber view, (B) apical two-chamber view and a cross sectional view at the level of the MA (C7) optimized in apical four- and two-chamber views. The yellow arrows help demonstrating the mitral annular plane in the long- (A,B) and short-axis (C7) images. Mitral annular dimensions including diameter (Dist), area (Area) and perimeter (Circ) are presented in the table (red D). RV, right ventricle; LV, left ventricle; RA, right atrium; LA, left atrium; MA, mitral annulus; dTGA, dextro-transposition of the great arteries.

function late after atrial switch operations (15-17). In earlier studies from the MAGYAR-Path Study, significant LA volumetric and functional abnormalities could be detected with more beneficial long-term effects for Senning-procedure compared to the Mustard-procedure (15). For RA, volumetric data were beneficial for Mustard-operated patients, while RA strains were more advantageous in subjects late after Senning-procedure suggesting some differences between the atria (16). In dTGA, dilated end-systolic and end-diastolic TA was found which was associated with deteriorated TA functional properties regardless of the atrial switch procedure performed (17). With known 3DSTE-derived normal reference values, in the present study, similar findings could be demonstrated for MA with dilated MA dimensions, which were associated with its impaired function (24). Senning-procedure showed (non-significant) beneficial findings during long-term (almost 30 years) follow-up.

The results demonstrated above are more interesting if we take it into consideration that dTGA patients had no significant MR. It is known that MA itself does not have contractility elements, its motion is highly dependent on the movement of adjacent atrial and ventricular

areas as demonstrated before even in healthy subjects without valvular regurgitations or stenoses (25-27). In recent studies, strong associations could be demonstrated between MA dimensions and functional properties and LV/LA parameters even in healthy subjects before valvular abnormalities develop (25-27). LA volumetric and functional abnormalities could be detected in dTGA following atrial switch (17) and compensatory LV morphological and functional changes and LV-RV interactions are theorized to maintain MA function, which could be a topic of future investigations.

In a recent study, Senning-operated subjects showed higher atrial strains as compared to that of Mustard-operated cases, which could be explained by the methodological differences between procedures when autologous native tissue is used during the Senning-procedure, while a synthetic material is used for the Mustard-procedure making the system more stiff theoretically (15). These could lead to MA functional differences, however, the effects of regional LV contractility could not be excluded either. These results could draw our attention to the late consequences of atrial switch operations for dTGA, comparative studies are warranted with subjects

who underwent arterial switch procedures.

### Limitation section

Hereby the most important limitations are listed:

- ❖ Only the projection of the MA to a selected 2D plane was assessed, not the real 3D saddle-shape of the MA.
- ❖ The image quality is known to be worse for 3DSTE as compared to that of 2D echocardiography, which could affect measured parameters and final results (8-12).
- ❖ Low number of dTGA patients who underwent atrial switch operation was enrolled in the present study due its infrequency (1-6). The analysis of more data would have been better, but there are no more patients available.
- ❖ Although 3DSTE is a suitable method for volumetric and strain assessments of atria and ventricles, detailed investigation of such parameters were not purposed (8-11).
- ❖ Validation of 3DSTE-derived variables were not purposed, as well. However, inter- and intraobserver variability data for MA parameters are given.
- ❖ There are limited information about 3DSTE-derived MA dimensions and functional properties, but their normal reference values together with their age- and gender-dependency has just been published (24).

### Conclusions

dTGA is accompanied by MA dilation and its functional impairment late after Senning- and Mustard-procedures.

### Acknowledgments

*Funding:* None.

### Footnote

*Provenance and Peer Review:* This article was commissioned by the Guest Editors (Yskert von Kodolitsch, Harald Kaemmerer and Koichiro Niwa) for the series “Current Management Aspects in Adult Congenital Heart Disease (ACHD): Part V” published in *Cardiovascular Diagnosis and Therapy*. The article has undergone external peer review.

*Reporting Checklist:* The authors have completed the STROBE reporting checklist. Available at <https://cdt.amegroups.com/article/view/10.21037/cdt-22-208/rc>

[amegroups.com/article/view/10.21037/cdt-22-208/rc](https://cdt.amegroups.com/article/view/10.21037/cdt-22-208/rc)

*Data Sharing Statement:* Available at <https://cdt.amegroups.com/article/view/10.21037/cdt-22-208/dss>

*Peer Review File:* Available at <https://cdt.amegroups.com/article/view/10.21037/cdt-22-208/prf>

*Conflicts of Interest:* Both authors have completed the ICMJE uniform disclosure form (<https://cdt.amegroups.com/article/view/10.21037/cdt-22-208/coif>). The series “Current Management Aspects in Adult Congenital Heart Disease (ACHD): Part V” was commissioned by the editorial office without any funding or sponsorship. The authors have no other conflicts of interest to declare.

*Ethical Statement:* The authors are accountable for all aspects of the work in ensuring that questions related to the accuracy or integrity of any part of the work are appropriately investigated and resolved. The study was conducted in accordance with the Declaration of Helsinki (as revised in 2013). The study was approved by the Institutional and Regional Human Biomedical Research Committee of University of Szeged, Hungary (No. 71/2011) and informed consent was taken from all individual participants.

*Open Access Statement:* This is an Open Access article distributed in accordance with the Creative Commons Attribution-NonCommercial-NoDerivs 4.0 International License (CC BY-NC-ND 4.0), which permits the non-commercial replication and distribution of the article with the strict proviso that no changes or edits are made and the original work is properly cited (including links to both the formal publication through the relevant DOI and the license). See: <https://creativecommons.org/licenses/by-nc-nd/4.0/>.

### References

1. Liebman J, Cullum L, Belloc NB. Natural history of transposition of the great arteries. *Anatomy and birth and death characteristics*. *Circulation* 1969;40:237-62.
2. Warnes CA. Transposition of the great arteries. *Circulation* 2006;114:2699-709.
3. Bravo-Valenzuela NJ, Peixoto AB, Araujo Júnior E. Prenatal diagnosis of transposition of the great arteries: an updated review. *Ultrasonography* 2020;39:331-9.
4. Gaur L, Cedars A, Diller GP, et al. Management

- considerations in the adult with surgically modified d-transposition of the great arteries. *Heart* 2021;107:1613-9.
5. Konstantinov IE, Alexi-Meskishvili VV, Williams WG, et al. Atrial switch operation: past, present, and future. *Ann Thorac Surg* 2004;77:2250-8.
  6. Haeffele C, Lui GK. Dextro-Transposition of the Great Arteries: Long-term Sequelae of Atrial and Arterial Switch. *Cardiol Clin* 2015;33:543-58, viii.
  7. Silbiger JJ. Anatomy, mechanics, and pathophysiology of the mitral annulus. *Am Heart J* 2012;164:163-76.
  8. Nemes A, Kalapos A, Domsik P, et al. Three-dimensional speckle-tracking echocardiography-- a further step in non-invasive three-dimensional cardiac imaging. *Orv Hetil* 2012;153:1570-7.
  9. Ammar KA, Paterick TE, Khandheria BK, et al. Myocardial mechanics: understanding and applying three-dimensional speckle tracking echocardiography in clinical practice. *Echocardiography* 2012;29:861-72.
  10. Urbano-Moral JA, Patel AR, Maron MS, et al. Three-dimensional speckle-tracking echocardiography: methodological aspects and clinical potential. *Echocardiography* 2012;29:997-1010.
  11. Muraru D, Niero A, Rodriguez-Zanella H, et al. Three-dimensional speckle-tracking echocardiography: benefits and limitations of integrating myocardial mechanics with three-dimensional imaging. *Cardiovasc Diagn Ther* 2018;8:101-17.
  12. Nemes A, Kovács Z, Kormányos Á, et al. The mitral annulus in lipedema: Insights from the three-dimensional speckle-tracking echocardiographic MAGYAR-Path Study. *Echocardiography* 2019;36:1482-91.
  13. Havasi K, Kalapos A, Berek K, et al. More than 50 years' experience in the treatment of patients with congenital heart disease at a Hungarian university hospital. *Orv Hetil* 2015;156:794-800.
  14. Havasi K, Kalapos A, Berek K, et al. Long-term follow-up of patients with transposition of the great arteries following Senning or Mustard operations. Results from the CSONGRAD Registry. *Orv Hetil* 2016;157:104-10.
  15. Nemes A, Rác G, Kormányos Á, et al. Left Atrial Volumetric and Deformation Analysis in Adult Patients with Dextro-Transposition of the Great Arteries (Insights from the CSONGRAD Registry and MAGYAR-Path Study). *J Clin Med* 2020;9:463.
  16. Nemes A, Kormányos Á, Ambrus N, et al. Features of the right atrium in repaired dextro-transposition of the great arteries following atrial switch operations (Insights from the CSONGRAD Registry and MAGYAR-Path Study). *Int J Cardiol Heart Vasc* 2022;38:100932.
  17. Nemes A, Rác G, Kormányos Á, et al. Tricuspid annular abnormalities in repaired dextro-transposition of the great arteries following Senning and Mustard procedures (Insights from the CSONGRAD Registry and MAGYAR-Path Study). *Cardiovasc Diagn Ther* 2021;11:1269-75.
  18. Lang RM, Badano LP, Mor-Avi V, et al. Recommendations for cardiac chamber quantification by echocardiography in adults: an update from the American Society of Echocardiography and the European Association of Cardiovascular Imaging. *Eur Heart J Cardiovasc Imaging* 2015;16:233-70.
  19. Anwar AM, Soliman OII, Nemes A, et al. Assessment of mitral annulus size and function by real-time 3-dimensional echocardiography in cardiomyopathy: comparison with magnetic resonance imaging. *J Am Soc Echocardiogr* 2007;20:941-8.
  20. Anwar AM, Soliman OII, ten Cate FJ, et al. True mitral annulus diameter is underestimated by two-dimensional echocardiography as evidenced by real-time three-dimensional echocardiography and magnetic resonance imaging. *Int J Cardiovasc Imaging* 2007;23:541-7.
  21. Silbiger JJ, Bazaz R. The anatomic substrate of mitral annular contraction. *Int J Cardiol* 2020;306:158-61.
  22. Mihaila S, Muraru D, Miglioranza MH, et al. Normal mitral annulus dynamics and its relationships with left ventricular and left atrial function. *Int J Cardiovasc Imaging* 2015;31:279-90.
  23. Camarda JA, Harris SE, Hambrook J, et al. Abnormal mitral valve anatomy in d-transposition of the great arteries: anatomic characterization and surgical outcomes. *Pediatr Cardiol* 2013;34:70-4.
  24. Nemes A, Kormányos Á, Domsik P, et al. Normal reference values of three-dimensional speckle-tracking echocardiography-derived mitral annular dimensions and functional properties in healthy adults: Insights from the MAGYAR-Healthy Study. *J Clin Ultrasound* 2021;49:234-9.
  25. Kovács Z, Kormányos Á, Domsik P, et al. Left ventricular longitudinal strain is associated with mitral annular fractional area change in healthy subjects-Results from the three-dimensional speckle tracking echocardiographic MAGYAR-Healthy Study. *Quant Imaging Med Surg* 2019;9:304-11.
  26. Domsik P, Kalapos A, Lengyel C, et al. Correlations between mitral annular and left atrial function as assessed by three-dimensional speckle-tracking echocardiography



- in healthy volunteers. Results from the MAGYAR-Healthy Study. *Orv Hetil* 2014;155:1517-23.
27. Nemes A, Kormányos Á, Ambrus N, et al. Associations between Mitral Annular and Left Atrial Volume Changes

in Healthy Adults—Detailed Analysis from the Three-Dimensional Speckle-Tracking Echocardiographic MAGYAR-Healthy Study. *Rev Cardiovasc Med* 2022;23:194.

**Cite this article as:** Nemes A, Kormányos Á. The mitral annulus in transposition of the great arteries late after Senning- and Mustard-procedures (Insights from the CSONGRAD Registry and MAGYAR-Path Study). *Cardiovasc Diagn Ther* 2022. doi: 10.21037/cdt-22-208